CRACK BRANCHING AND THRESHOLD CONDITIONS OF SMALL CRACKS IN BIAXIAL FATIGUE

Y. Murakami* and K. Takahashi*

In this work the threshold condition for fatigue limit of materials, containing small cracks, under biaxial stress has been studied. Biaxial fatigue tests have been carried out on 0.47% C steel specimens containing an initial small crack. The initial small semi-elliptical cracks of 400μm were introduced by a prior tension-compression fatigue test using specimens containing a 40μm diameter hole. The crack growth behaviour from a semi-elliptical surface crack has been investigated. The fatigue limit under biaxial stress is determined from a threshold condition for non-propagation of Mode I branched cracks. The test results are compared with the maximum tangential stress criterion.

INTRODUCTION

Problems of small cracks in biaxial or multiaxial fatigue have recently been studied (1,2). Murakami et al. (3-5) studied systematically the effects of small defects and cracks in rotating bending and tension-compression fatigue and proposed a prediction model named "the $\sqrt{area}$ parameter model". Effects of artificial small defects on torsional fatigue strength have been also studied based on the same model (6-8). Recently, based on the model, small crack effects on torsional fatigue strength have been investigated (9). It has been recognized in existing literature that analyzing the behaviour of small cracks is the key to solving the problems of multiaxial fatigue.

Several studies have been carried out to investigate the threshold behaviour of a crack under biaxial loading (10,11); though the crack length in these studies was not small enough to deduce the behaviour of small cracks. In this study, the threshold behaviour under biaxial loading has been investigated on 0.47% C steel specimens containing an initial small crack of 400μm in surface length.

PREDICTION OF FATIGUE LIMIT IN ROTATING BENDING AND TORSION

The authors, in the previous studies, conducted rotating bending (12) and torsional

Dept. of Mechanical Science and Engineering, Kyushu University, Fukuoka, Higashi-ku, 812-8581 Japan

(9) fatigue tests on annealed 0.46~0.47%C steel using specimens containing an initial small semi-elliptical crack ranging from 200μm to 1300μm. Figure 1 shows the fatigue limit as a function of crack size ($\sqrt{area}$) in rotating bending and reversed torsion of 0.46~0.47%C steel under zero mean stress (R=-1).

"The $\sqrt{area}$ parameter model" for predicting rotating-bending or tension-compression fatigue limit (σ_w) of materials containing a small surface defect and a small surface crack is expressed as follows (3-5).

$$\sigma_w = 1.43(HV + 120) \Big/ (\sqrt{area})^{\frac{1}{6}} \quad (1)$$

,where σ_w is in MPa under R=-1, HV is Vickers hardness number in kgf/mm^2 and $\sqrt{area}$ is in μm.

Murakami and Takahashi (9) showed that the fatigue limit of cracked specimens, under reversed torsion (R=-1), is the threshold condition for non-propagation of Mode I branched crack. Figure 2 shows the branching of cracks by torsion from an initial crack which was introduced by prior tension-compression fatigue. Experimentally observed branching angles (θ_0) are larger than ±45° of the direction of nominal maximum principal stress and rather close to ±70.5° which is the direction of the local maximum tangential stress at crack tip. Thus, applying the maximum tangential stress criterion to the initial crack tip in combination with the $\sqrt{area}$ parameter model, the torsional fatigue limit (τ_w) can be calculated by (9)

$$\tau_w = \frac{0.93}{F(b/a)}(HV + 120) \Big/ (\sqrt{area_p})^{\frac{1}{6}}$$

$$F(b/a) = 0.0957 + 2.11(b/a) - 2.26(b/a)^2 + 1.09(b/a)^3 - 0.196(b/a)^4 \quad (2).$$

,where τ_w is in MPa under R=-1, HV is in kgf/mm^2. The geometrical parameter, $\sqrt{area_p}$(μm), is defined by the square root of the area of a pre-crack projected onto a plane perpendicular to the maximum principal stress, i.e. ±45° to the specimen axis under cyclic torsion.

MATERIAL AND TEST PROCEDURE

The material used was a rolled 25mm diameter bar of 0.47%C steel (S45C). The chemical composition is (wt.%) 0.47C, 0.21Si, 0.82Mn, 0.018P, 0.018S, 0.01Cu, 0.018Ni and 0.064Cr. The mechanical properties of material are 620MPa tensile strength, 339MPa lower yield strength, 1105MPa true fracture strength and 53.8% reduction of area. Specimens were made by turning after annealing at 844℃ for 1hr. The specimen diameter is 8mm and the test length is 20mm. After surface finishing with an emery paper, about 25μm of surface layer was removed by electropolishing. A hole of 40μm diameter/depth was then introduced onto the surface of each specimen. Specimens were then annealed in a vacuum at 600℃ for 1hr to relieve residual stress caused by drilling. The Vickers hardness after vacuum annealing was HV=178 which is a mean value of each specimen measured at 4 points with load of 0.98N. The scatter in HV was within 5%.

A hydraulic controlled biaxial testing machine was used for introduction of pre-crack by tension-compression followed by a torsional fatigue test. Tension-compression fatigue tests were conducted at σ=230MPa, to introduce pre-cracks of 400μm in surface length including a hole. The frequency of the test was 20Hz with R=-1. SEM observation of fracture surface identified that pre-cracks were semi-elliptical and the mean value of aspect ratios (b/a) was 0.9.

These specimens were annealed in a vacuum at 600℃ for 1hr again to relieve prior fatigue history caused by the tension-compression fatigue. Then, in-phase biaxial fatigue tests were conducted under load control at a frequency of 12Hz with R=-1. Fatigue tests were carried out at constant stress amplitude ratio, τ_a/σ_a=0.8 and 2.0. The fatigue limit was defined by the maximum nominal stress under which a specimen endured 10^7 cycles. The minimum test step of stress level is 4.9MPa. Plastic replicas were taken from the specimen surface during the tests to monitor crack growth.

RESULTS AND DISCUSSION

Crack Growth and Threshold Condition of Small Cracks under Biaxial Stress

Figure 3(a) shows cracks branched by Mode I in τ_a/σ_a=2.0 from the tip of initial crack under a stress level higher than fatigue limit. Mode I crack continued to propagate and led to specimen failure. Figure 3(b) shows the shape and angle of a branched crack. The branched cracks propagated eventually in a direction perpendicular to the principal stresses for τ_a/σ_a=2.0, i.e. -38.0° against initial crack, though the initial branching angle is obviously larger than -38.0° and close to -61.4° which is the direction of the local maximum tangential stress.

Cracks which branched at a stress below the fatigue limit stopped propagating. Figure 3(c) shows a non-propagating crack at fatigue limit. Thus, the fatigue limit under biaxial stress is the threshold condition for non-propagation of Mode I branched cracks as well as cyclic torsion (9).

Application of the Maximum Tangential Stress Criterion

Based on the experimental observations that the threshold condition is determined by the local stress field at crack tip, the threshold condition under biaxial stress is evaluated using the threshold stress intensity factor range (ΔK_{th}) for Mode I small cracks. Stress intensity factor range ($\Delta K_{\theta max}$) which prescribes the local field of the maximum tangential stress ($\sigma_{\theta max}$) at crack tip is defined by

$$\Delta K_{\theta\,max} = \Delta\sigma_{\theta\,max}\sqrt{2\pi r}$$

$$= \cos\frac{\theta_0}{2}\left[\Delta K_I \cos^2\frac{\theta_0}{2} - \frac{3}{2}\Delta K_{II}\sin\theta_0\right] \quad (3).$$

,where ΔK_I and ΔK_{II} are stress intensity factor ranges of an initial crack defined by the following equations.

$$\Delta K_I = F_I \Delta\sigma\sqrt{\pi a} \quad (4)$$

$$\Delta K_{II} = F_{II}\Delta\tau\sqrt{\pi a} \quad (5)$$

,where F_I and F_{II} are the dimensionless correction factor, $\Delta\sigma$=2σ_a, $\Delta\tau$=2τ_a and 2a is surface crack length. The angle θ_0 in Eq.(3) is that of the local polar coordinate (r,θ) with the origin at crack tip where σ_θ has the maximum value. The value of θ_0 is obtained by the following equation (13).

$$\Delta K_I \sin\theta_0 + \Delta K_{II}(3\cos\theta_0 - 1) = 0 \quad (6)$$

The maximum value of stress intensity factor (K_{Imax}) along the front of a surface crack of arbitrary shape subjected to remote tensile stress (σ_0) is given by (14)

$$K_{Imax} \cong 0.65\sigma_0\sqrt{\pi\sqrt{area}} \quad (7)$$

F_I for a semi-elliptical surface crack with aspect ratio b/a=0.9 is obtained by

substituting Eq.(7) with $area=1/2\pi ab,(b=0.9a)$ to Eq.(4). F_{II} is approximately calculated by Kassir and Sih's solution (15) for an elliptical crack in an infinite body under remote uniform shear stress. ΔK_{th} for various metals containing a small crack or defect is given as follows by the $\sqrt{area}$ parameter model (3-5).

$$\Delta K_{th} = 3.3\times10^{-3}(HV+120)\left(\sqrt{area}_p\right)^{\frac{1}{3}} \tag{8}$$

,where ΔK_{th} is in MPa$\sqrt{}$m under R=-1, HV is Vickers hardness number in kgf/mm^2 and $\sqrt{area}_p$ (μm) is the square root of the area of an inclined crack projected onto a plane perpendicular to the maximum tensile stress. The direction of maximum tensile stress depends on the ratio τ_a/σ_a. Therefore, the value of $\sqrt{area}_p$ varies depending on the ratio τ_a/σ_a. It is assumed that at the threshold $\Delta K_{\theta max}$ is equal to ΔK_{th} in Mode I. Substituting Eq.(8) and Eqs.(4) and (5) to Eq.(3), fatigue limit (σ_w, τ_w) can be obtained for each stress amplitude ratio τ_a/σ_a.

Figure 4 shows experimental results and predictions. Prediction of (σ_w, τ_w) is shown by the solid line in Fig.4. In simple tension-compression fatigue and pure reversed torsional fatigue, predictions obtained by Eqs.(1) and (2) are in good agreement with experimental results (9,12). However, in general mixed-mode loadings, predictions are conservative. This is due to friction between the initial crack surfaces. Figure 5 shows debris that appeared on the specimen surface due to rubbing between crack surfaces by shear under a compressive stress. Thus, the friction at crack surfaces makes an effective value of $\Delta K_{\theta max}$ less than the applied nominal value of $\Delta K_{\theta max}$. The effect of rubbing is thought to increase with increasing the product of τ_a and the absolute value of compressive stress $|\sigma_a|$, i.e. $|\tau_a\sigma_a|$.

Regarding the threshold condition of initiation of a branching crack from a long 2D crack (longer than 10mm), Gao et al. (10) conducted fatigue crack growth tests on AISI 316 stainless steel under mixed-mode I and II loading. They showed that threshold condition for initiation of Mode I branched crack depends on contact and rubbing at the crack surface. Pook (11) constructed a theoretical lower bound of initiation threshold for Mode I branched crack based on the maximum tangential stress criterion and confirmed it experimentally. However, in these studies, the threshold condition for crack initiation and not for non-propagation is discussed in terms of long cracks.When we discuss the fatigue limit under biaxial loading, we must pay attention to the non-propagation condition as the fatigue threshold. Furthermore, it must be noted that the threshold condition for small cracks under torsion or biaxial loading is essentially a function of crack size as shown in the present study as well as the case of Mode I.

CONCLUSION

(1)The branched cracks propagated eventually in the direction perpendicular to the maximum principal stress, though the initial branching angle is obviously larger than that and close to the direction of the local maximum tangential stress.

(2)Fatigue limit of small cracks under biaxial stress is determined by the Mode I threshold condition for non-propagation of branched cracks

(3)Fatigue limit under mixed-mode stress was predicted by the $\sqrt{area}$ parameter model with the maximum tangential stress criterion. In simple tension-compression fatigue and pure torsional fatigue, predictions are in good agreement with experimental results. However, in general mixed-mode loadings, predictions are conservative due to friction between initial crack surfaces.

REFERENCES

(1) Brown, M. W. and Miller, K.J., "Biaxial and Multiaxial Fatigue", Mech. Engng Publ. Ltd., London, 1989.

(2) Leese, G. E. and Socie, D. F., "Multiaxial Fatigue : Analysis and Experiments", Society of Automotive Engineers, Inc., Pennsylvania, 1989.

(3) Murakami, Y. and Endo, M., "The Behaviour of Short Fatigue Cracks", EGF1, Edited by Miller, K. J. and de los Rios, E. R., Mech. Engng. Publ., London, 1986, pp.275-293.

(4) Murakami, Y. "Metal Fatigue:Effects of Small Defects and Nonmetallic Inclusion on Fatigue Strength", Yokendo Ltd, Japan 1993.

(5) Murakami, Y. and Endo, M., Int. J. Fatigue, Vol.16, 1994, pp.163-182.

(6) Endo, M. and Murakami, Y., J. Engng Mater. Tech., Trans. ASME, Vol.109, 1987, pp.124-129.

(7) Endo, M., J. Soc. Mater. Sci., Japan, Vol.45, 1996, pp.16-20.

(8) Murakami, Y., Takahashi, K., Takada, M. and Toriyama, T., Trans. Jpn. Soc. Mech. Engnrs, Ser.A, Vol.64, No.618, 1998, pp.271-277.

(9) Murakami, Y. and Takahashi, K., Submitted to Fatigue Fract. Engng Mater. Struct. 1998.

(10) Gao Hua, Brown, M. W. and Miller, K. J., Fatigue Fract. Engng Mater. Struct. Vol.5, 1982, pp.1-17.

(11) Pook, L.P., "Biaxial and Multiaxial Fatigue", EGF3, Edited by Brown, M. W. and Miller, K. J., Mech. Engng. Publ., London, 1989, pp.247-263.

(12) Murakami, Y. and Matsuda, K. Trans. Jpn. Soc. Mech. Engnrs, Ser.A, Vol.52, No.478, 1986, pp.1492-1499.

(13) Erdogan,F. and Sih,G.C., J. Bas. Engng, Trans. ASME Vol.85, 1963, pp.519-527.

(14) Murakami, Y. and Isida, M., Trans.Jpn.Soc.Mech. Engnrs, Ser.A, Vol.51, No.464, 1985, pp.1050-1056.

(15) Kassir, M. K. and Sih, G. C., J. Appl. Mech., Trans. ASME Vol.33, 1966, pp.601-611. In: "Stress Intensity Factors Handbook ", Murakami, Y. et al. (eds.), Vol.2, pp.686-689. Pergamon Press, 1987.

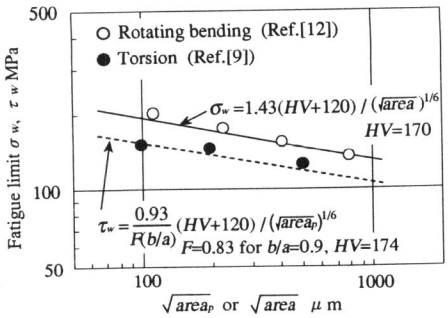

Figure 1 Relationship between rotating bending fatigue limit (σ_w) and torsional fatigue limit (τ_w) and $\sqrt{area}$ under zero mean stress (R=-1). 0.46~0.47% carbon steel.

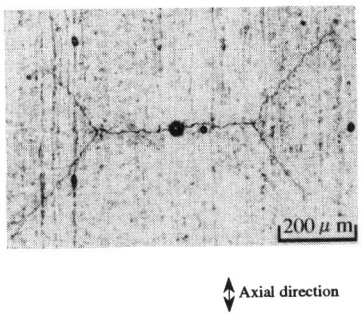

Figure 2 Propagation of branched cracks in cyclic torsion (R=-1) . τ_a=152MPa, N=4.0×10^5, N_f=7.9×10^5.

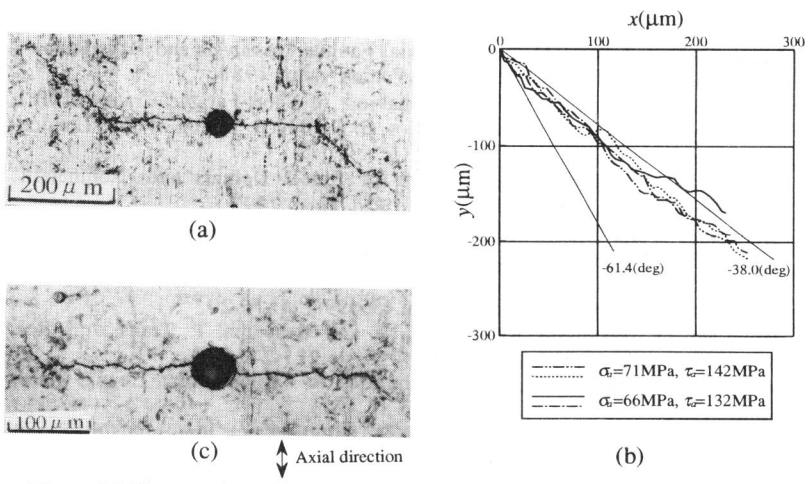

Figure 3 (a)Propagation of branched cracks. σ_a=71MPa, τ_a=142MPa, τ_a/σ_a=2.0, N=1.5×10^5, N_f=3.8×10^5. (b)Shape and angle of the branched crack, τ_a/σ_a=2.0. (c)Non-propagating cracks observed at fatigue limit . σ_w=64 MPa, τ_w=127MPa, τ_w/σ_w=2.0.

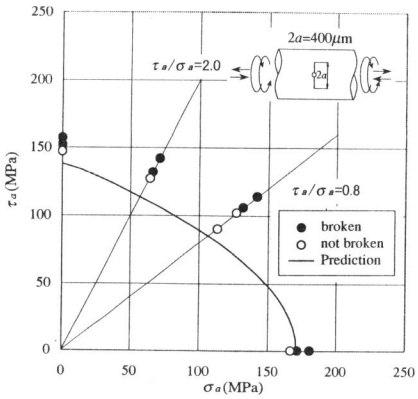

Figure 4 Comparison of predictied fatigue limits with experimental results.

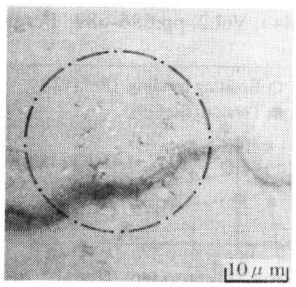

Figure 5 Debris appeared on the surface due to rubbing between crack surfaces. τ_w/σ_w=0.8, σ_w=127MPa, τ_w=102MPa, N=1.0×10^7.